

Figure 8 Measured radiation patterns at 1.575 GHz for the prototype with $C = 0.9$ pF. (a) x - z plane and (b) y - z plane

1.575 GHz is about 1%. Furthermore, it is found that when C is varied between 0.8 and 1.0 pF, the requirements including return loss of less than 10 dB and axial ratio of lower than 3 dB can still be achieved at 1.575 GHz. This implies that the CP performances of the proposed design are not very sensitive to the capacitance value of the lumped capacitors. The radiation patterns are also measured, and the results at 1.575 GHz are plotted in Figure 8. Broadside radiations with wide 3 dB-axial-ratio beamwidth are seen in the x - z and y - z planes. The front-to-back ratio is higher than 10 dB. Due to the compact antenna structure and lossy substrate, the peak gain is about 0.5 dB.

4. CONCLUSION

A compact design for CP microstrip antennas has been presented. The design is the integration of a square-ring patch antenna and a quasilumped quadrature coupler. A prototype operating at the GPS band was implemented on a commercial FR4 substrate of thickness 1.6 mm, and the required area for the radiating patch and the coupler is about $39 \text{ mm} \times 39 \text{ mm}$. The area would be further reduced by enlarging the inner slot of the ring patch and simultaneously selecting a larger system impedance of the coupler.

REFERENCES

1. M. Chen and C.C. Chen, A compact dual-band GPS antenna design, *IEEE Antennas Wireless Propagat Lett* 12 (2013), 245–248.
2. A. Hoorhar and A. Perrotta, An experimental study of microstrip antennas on very high permittivity ceramic substrates and very small ground plane, *IEEE Trans Antennas Propagat* 49 (2001), 838–840.
3. X. Nasimuddin, X. Qing, and Z.N. Chen, Compact asymmetric-slit microstrip antennas for circular polarization, *IEEE Trans Antennas Propagat* 59 (2011), 285–288.
4. T.C. Yo, C.M. Lee, C.M. Hsu, and C.H. Luo, Compact circularly polarized rectenna with unbalanced circular slots, *IEEE Trans Antennas Propagat* 56 (2008), 882–886.
5. X.L. Bao and M.J. Ammann, Compact annular-ring embedded circular patch antenna with cross-slot ground plane for circular polarisation, *Electron Lett* 34 (2006), 192–193.
6. J.S. Row and C.Y. Ai, Compact design of a single-feed circularly polarised microstrip antenna, *Electron Lett* 40 (2004), 1093–1094.

7. F. Ferrero, C. Luxey, R. Staraj, G. Jacquemod, M. Yedlin, and V. Fusco, A novel quad-polarization agile patch antenna, *IEEE Trans Antennas Propagat* 57 (2009), 1562–1566.
8. J.S. Row, Design of square-ring microstrip antenna for circular polarisation, *Electron Lett* 40 (2004), 93–94.
9. T.Y. Han, C.J. Shih, and J.S. Row, Polarization reconfigurable microstrip patch antenna, *Microwave Opt Technol Lett* 55 (2013), 471–474.

© 2014 Wiley Periodicals, Inc.

COUPLED-FED INVERTED-F ANTENNA USING AN INVERTED-F COUPLING FEED FOR SMALL-SIZE LTE/WWAN TABLET COMPUTER ANTENNA

Kin-Lu Wong and Li-Yu Chen

Department of Electrical Engineering, National Sun Yat-sen University, Kaohsiung, 80424, Taiwan, People's Republic of China; Corresponding author: wongkl@ema.ee.nsysu.edu.tw

Received 1 October 2013

ABSTRACT: A coupled-fed inverted-F antenna for small-size dual-wideband operation in the mobile communication devices, especially the slim tablet computers, for the long term evolution/wireless wide area network (LTE/WWAN) operation, is proposed. The antenna comprises a folded radiating strip and an inverted-F coupling feed. The former is grounded to the device ground plane and is capacitively excited by the inverted-F coupling feed. Two wide operating bands to cover the LTE/WWAN operation in the 704~960 and 1710~2690 MHz bands are generated for the antenna. In addition, the antenna's metal pattern has a planar structure and occupies a small area of $10 \times 40 \text{ mm}^2$ on a 0.4-mm thick FR4 substrate. Operating principle and design considerations of the proposed antenna to generate the dual-wideband operation are addressed. Experimental results of the fabricated antenna are also presented and discussed. © 2014 Wiley Periodicals, Inc. *Microwave Opt Technol Lett* 56:1296–1302, 2014; View this article online at wileyonlinelibrary.com. DOI 10.1002/mop.28334

Key words: mobile antennas; inverted-F antennas; LTE/WWAN antennas; tablet; computer antennas; coupled-fed antennas

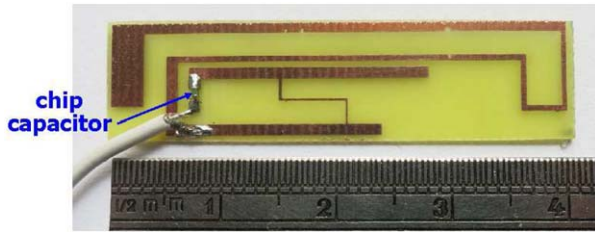


Figure 2 Photo of the fabricated antenna. [Color figure can be viewed in the online issue, which is available at wileyonlinelibrary.com]

to achieve the dual-wideband operation to cover the LTE/WWAN bands in the slim tablet computers. The antenna size is $10 \times 40 \text{ mm}^2$ only and can be disposed on one surface of a 0.4-mm thick FR4 substrate. In the proposed design, the single-branch radiator is a folded strip grounded to the device ground plane of the tablet computer, while the inverted-F coupling feed capacitively excites the folded strip to generate a fundamental resonant mode in the lower band and a higher-order resonant mode in the higher band. Then, by adjusting the length of the shorting strip and embedding a proper chip capacitor in the feeding strip of the inverted-F coupling feed, dual-wideband operation for the antenna to cover the LTE/WWAN operation including the LTE700/GSM850/900 (704~960 MHz) bands and GSM1800/1900/UMTS/LTE2300/2500 (1710~2170/2300~2400/2500~2690 MHz) bands can be obtained. Operating principle of the proposed antenna is described, and design considerations of the antenna to generate the dual-wideband operation are addressed. The antenna was also fabricated and tested, and results of the fabricated antenna are presented.

2. PROPOSED ANTENNA AND PARAMETRIC STUDY

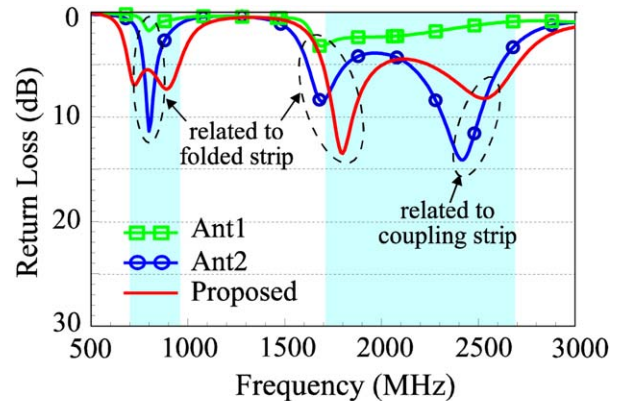
Figure 1 shows the geometry of the proposed LTE/WWAN coupled-fed inverted-F antenna for the tablet computer applications. The antenna has a planar structure and is disposed on one surface of a thin FR4 substrate, which has a size of $10 \times 40 \times 0.4 \text{ mm}^3$, a relative permittivity of 4.4, and a loss tangent of 0.024. The antenna is formed by a folded radiating strip (section HI in the figure) and an inverted-F coupling feed, with the latter capacitively exciting the former through a coupling gap (g) of 0.5 mm. The folded strip having a length of 94 mm is configured into a compact structure and short-circuited to a small ground pad of size $1 \times 20 \text{ mm}^2$, which is connected to the device ground plane of dimensions $150 \times 200 \text{ mm}^2$. The ground plane dimensions are selected for the consideration of a practical tablet computer with a 9.7-in. display panel, which is popular on the market. To feed the antenna in the experiment, a 50- Ω coaxial line is applied (see the photo of the fabricated antenna in Fig. 2), with its central conductor and outer grounding sheath connected to point A at the coupling feed and point B at the ground pad, respectively.

The antenna's operating principle is first analyzed. Figure 3 shows the simulated return loss for the proposed antenna, the case without the shorting strip and the chip capacitor in the feeding strip of the coupling feed (Ant1), and the case without the chip capacitor in the feeding strip of the coupling feed (Ant2). The simulated results are obtained using the EM field simulator HFSS version 14 [6]. In the figure, the two shaded frequency ranges represent the desired frequency bands of 704~960 and 1710~2690 MHz. The corresponding results of the simulated input impedance of Ant1 and Ant2 are also presented in Figure 4(a), while those for the proposed antenna and

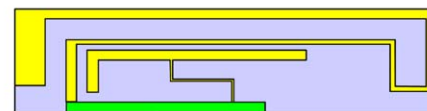
Ant2 are shown in Figure 4(b). From the results in Figure 3, it is noted that there are two resonant modes excited at about 800 and 1700 MHz for Ant1, with the lower and higher resonant modes being the fundamental and higher-order resonant modes of the folded strip, respectively. However, the impedance matching of the two resonant modes is poor for practical applications.

When the shorting strip (section DE, length 10 mm) is added to Ant1 to form Ant2, the impedance matching of the two resonant modes is greatly improved. This is mainly because the added shorting strip leads to the generation of a parallel-resonance excitation [7, 8] at about 1.3 GHz [see Fig. 4(a)], which improves the impedance matching of the folded strip's fundamental resonant mode. Good excitation of the folded strip's higher-order resonant mode at about 1.7 GHz is also obtained owing to the presence of the shorting strip. In addition, a new resonant mode at about 2.5 GHz contributed by the coupling strip (section FG, length 21 mm) is generated, which is owing to the shorting strip that short-circuits the coupling strip to the ground pad to compensate for the strong coupling between the coupling strip and the device ground plane. In this case, the inverted-F coupling feed also forms an effective radiator to contribute a resonant mode at higher frequencies to greatly widen the antenna's high-band bandwidth. Note that the resonant mode contributed by the inverted-F coupling feed can be easily tuned by adjusting the length t of the coupling strip, which will be discussed with aid of Figure 6 later.

By further adding a chip capacitor of 2 pF to the feeding strip of Ant2, the proposed antenna is formed. In this case, as shown in Figure 3, two wide operating bands to cover the

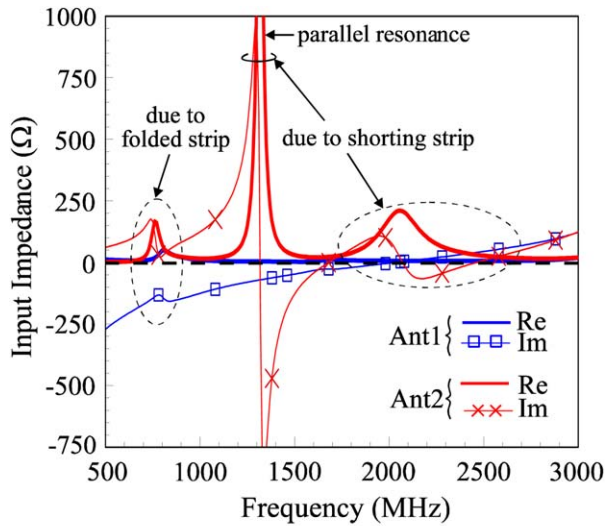


Ant1 (no shorting strip and chip capacitor)

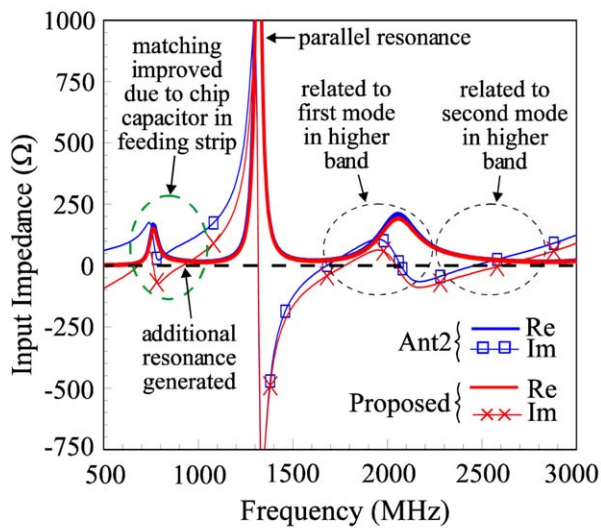


Ant2 (no chip capacitor)

Figure 3 Simulated return loss for the proposed antenna, the case without the shorting strip and the chip capacitor in the feeding strip of the coupling feed (Ant1), and the case without the chip capacitor in the feeding strip of the coupling feed (Ant2). [Color figure can be viewed in the online issue, which is available at wileyonlinelibrary.com]



(a)



(b)

Figure 4 Comparison of simulated input impedance for (a) Ant1 and Ant2 in Figure 3 and (b) the proposed antenna and Ant2 in Figure 3. [Color figure can be viewed in the online issue, which is available at wileyonlinelibrary.com]

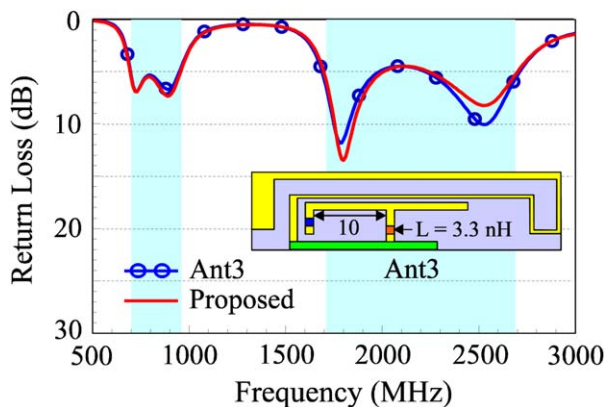


Figure 5 Simulated return loss for the proposed antenna and the case using a chip-inductor-loaded shorting strip in the inverted-F coupling feed (Ant3). Other parameters are the same as in Figure 1. [Color figure can be viewed in the online issue, which is available at wileyonlinelibrary.com]

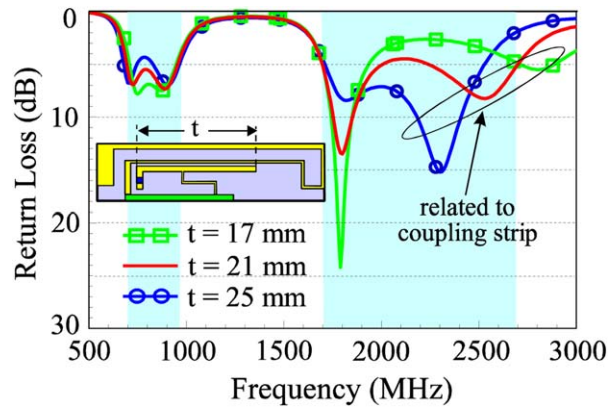


Figure 6 Simulated return loss as a function of the length t of the coupling strip. Other parameters are the same as in Figure 1. [Color figure can be viewed in the online issue, which is available at wileyonlinelibrary.com]

desired 704~960 and 1710~2690 MHz bands are obtained. This is mainly because the added chip capacitor can be considered like a high-pass matching circuit to compensate for the large inductive reactance of the folded strip's fundamental resonant mode of Ant2, with small effects on the parallel resonance at about 1.3 GHz and the resonant modes at higher frequencies [see Fig. 4(b)]. The impedance matching improvement of the folded strip's fundamental resonant mode further causes an additional resonance occurred at about 900 MHz in the high-frequency portion thereof. In this case, a new resonant mode owing to the additional resonance is generated, which combines with the folded strip's fundamental resonant mode to greatly widen the antenna's low-band bandwidth. In addition, please note that although the return loss for part of the frequencies in the desired operating bands is not better than 6 dB, the measured antenna efficiency (with mismatching loss included) is all better than 50% in both the lower and higher bands (see Fig. 11 in Section 3), which is acceptable for practical mobile communication applications [9, 10].

From the results in Figures 3 and 4, it indicates that both the embedded chip capacitor and the shorting strip have combined effects in achieving bandwidth enhancement of the antenna's lower and higher bands. Also note that the shorting strip is configured into a step shape to have a length of 10 mm, which can provide an equivalent inductance of about 3.3 nH. This can be

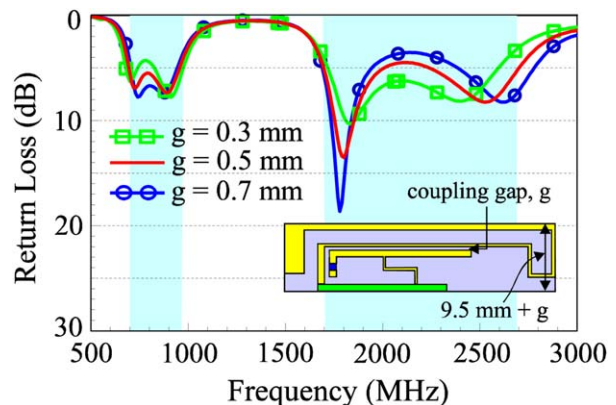


Figure 7 Simulated return loss as a function of the coupling gap g between the folded strip and the coupling strip. [Color figure can be viewed in the online issue, which is available at wileyonlinelibrary.com]

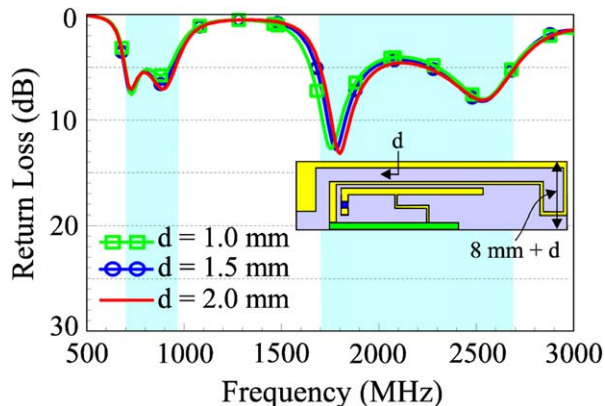


Figure 8 Simulated return loss as a function of the spacing d in the folded strip. [Color figure can be viewed in the online issue, which is available at wileyonlinelibrary.com]

confirmed from the simulated return loss for the proposed antenna and Ant3 (the case using a short, simple shorting strip loaded with a chip inductor of 3.3 nH to replace the step-shaped shorting strip in the proposed antenna) shown in Figure 5, in which the proposed antenna and Ant3 show very similar results. This also suggests that by adjusting the length of the shorting strip, which leads to different equivalent inductance provided [11, 12], the wideband characteristics of the antenna's two operating bands can be adjusted.

In addition to the embedded chip capacitor and the shorting strip, some parameters of the proposed antenna are also ana-

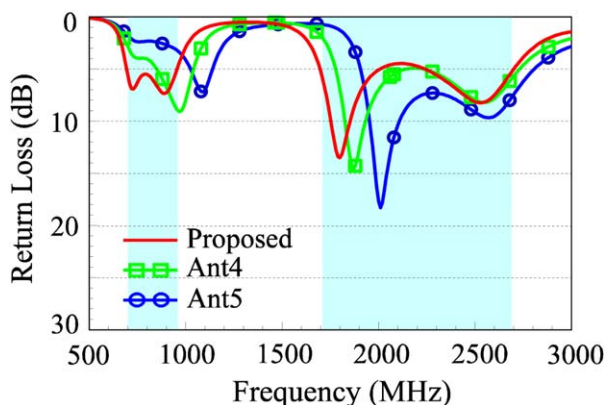


Figure 9 Simulated return loss for the proposed antenna with different lengths of the folded strip (Ant4 and Ant5). Other parameters are the same as in Figure 1. [Color figure can be viewed in the online issue, which is available at wileyonlinelibrary.com]

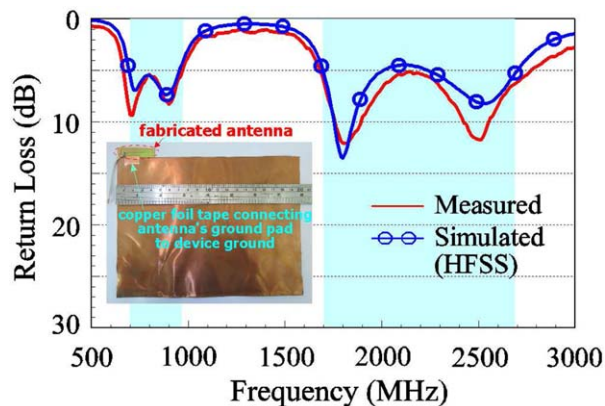


Figure 10 Measured and simulated return loss of the fabricated antenna. [Color figure can be viewed in the online issue, which is available at wileyonlinelibrary.com]

lyzed. Figure 6 shows the simulated return loss as a function of the length t of the coupling strip (section FG in Fig. 1). Other parameters are the same as in Figure 1. Results of the length t varied from 17 to 25 mm are shown. Large effects on the second mode of the antenna's higher band are seen, which is shifted to lower frequencies with an increase in the length t . At the same time, relatively small effects on the other resonant modes are seen. This suggests that by tuning the length of the coupling strip, the antenna's high-band bandwidth can be adjusted.

Figure 7 shows the simulated return loss as a function of the coupling gap g between the folded strip and the coupling strip. Results for the coupling gap varied from 0.3 to 0.7 mm are shown. Note that for the results shown in Figure 7, the parameters of the folded strip and inverted-F coupling feed are the same as in Figure 1, while the antenna height is varied to be 9.8, 10, and 10.2 mm for $g = 0.3, 0.5,$ and 0.7 mm, respectively. Since the folded strip's fundamental resonant mode and higher-order resonant mode are capacitively excited by the inverted-F coupling feed through the coupling gap g , some effects are seen when the coupling gap g is varied. Hence, the coupling gap should also be fine-tuned to achieve acceptable impedance matching for the dual-wideband operation.

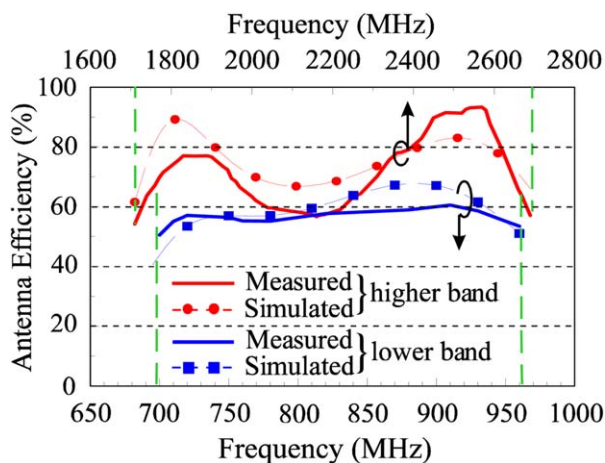


Figure 11 Measured and simulated antenna efficiency (matching loss included) of the fabricated antenna. [Color figure can be viewed in the online issue, which is available at wileyonlinelibrary.com]

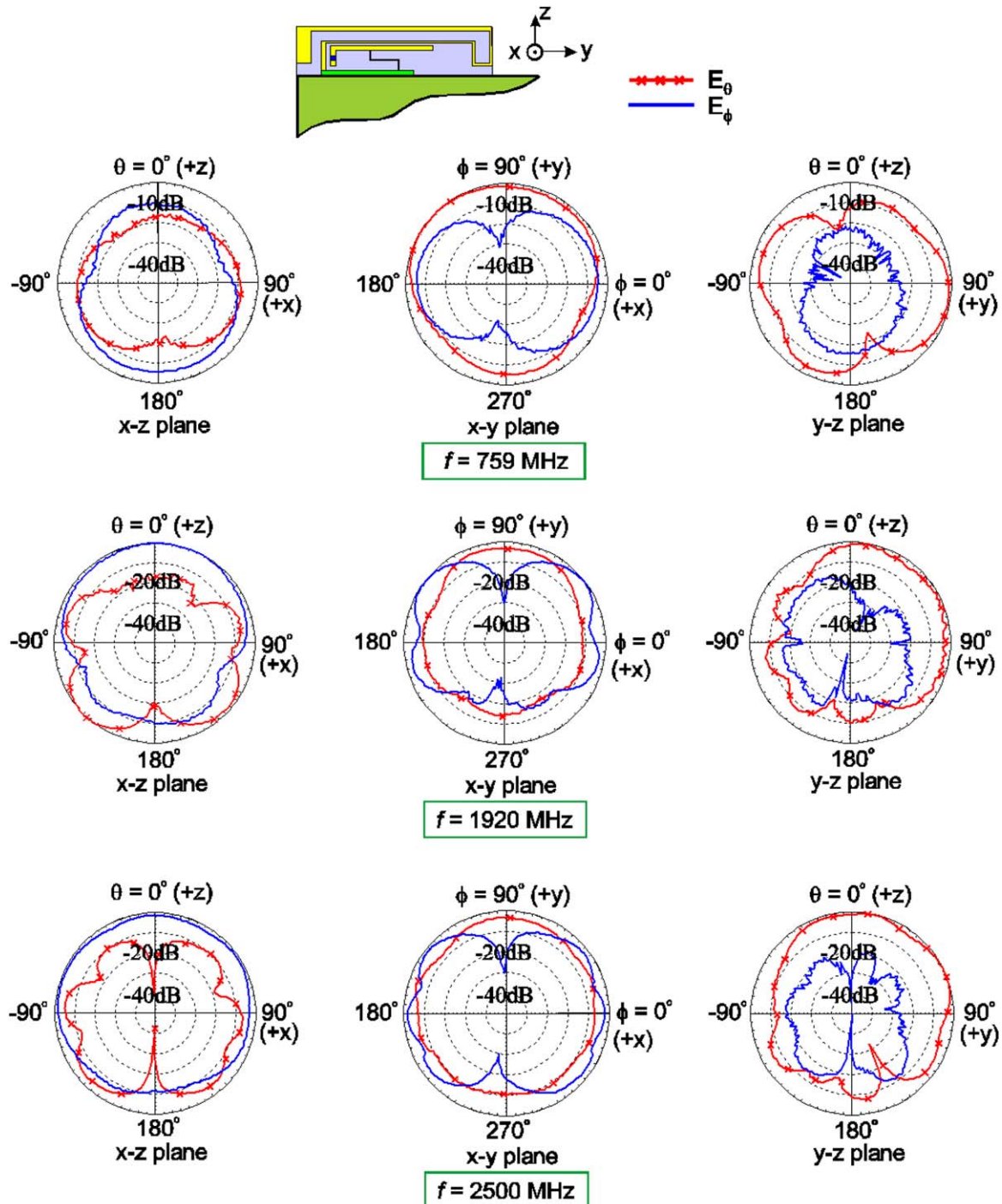


Figure 12 Measured radiation patterns at 759, 1920, and 2500 MHz of the fabricated antenna. [Color figure can be viewed in the online issue, which is available at wileyonlinelibrary.com]

Effects of the spacing d between adjacent sections of the folded strip are also studied. Results of the spacing d varied from 1.0–2.0 mm are shown in Figure 8. In this case, note that with other parameters the same as in Figure 1, the antenna height is varied to be 9.0, 9.5, and 10 mm for $d = 1.0$, 1.5, and 2.0 mm, respectively. Although smaller spacing d ($d = 1.0$ and 1.5 mm) can lead to a decreased antenna height, the impedance matching of the frequencies in the antenna's lower band is degraded, especially for the case with $d = 1.0$ mm, which will decrease the antenna's low-band bandwidth.

In the proposed antenna, the spacing d is hence selected to be 2.0 mm.

Effects of varying the length of the folded strip are also studied. Results of the simulated return loss for the length of the folded strip varied to be 87 mm (Ant4) and 80 mm (Ant5) are shown in Figure 9, and other parameters are the same as in Figure 1. Large effects on the antenna's lower band and the first resonant mode in the higher band are seen. This is reasonable since the two resonant modes in the lower band are related to the folded strip's fundamental resonant mode and the first

resonant mode in the higher band is the folded strip's higher-order resonant mode, while the resonant mode at about 2.5 GHz is related to the inverted-F coupling feed. Also note that in the proposed antenna, the folded strip is selected to have a length of 94 mm (corresponding to be about 0.25 wavelength of the frequency at 800 MHz) and is configured into a compact size such that the proposed antenna can be disposed on a thin FR4 substrate of $10 \times 40 \times 0.4 \text{ mm}^3$, which is smaller than many reported LTE/WWAN operations for the tablet computer or notebook computer applications [2, 4, 5, 13–21].

3. EXPERIMENTAL RESULTS AND DISCUSSION

The fabricated antenna shown in Figure 2 is tested with its ground pad connected to the device ground plane using a copper foil tape (see the photo inset in Figure 10), which is used in some practical notebook or tablet computer applications. In the experiment, the device ground plane was cut from a 0.2-mm thick copper plate. Results of the measured and simulated return loss of the fabricated antenna shown in Figure 10 are in good agreement. Two wide operating bands are obtained to cover the 704~960 and 1710~2690 MHz bands for the LTE/WWAN operation.

Figure 11 shows the measured and simulated antenna efficiency of the fabricated antenna. The antenna efficiency includes the mismatching losses, and measured results also in general agree with the simulated results. For frequencies over the desired lower and higher bands, the measured antenna efficiency is about 50~61% and 55~94%, respectively, which is acceptable for practical applications [9, 10]. Figure 12 shows the measured radiation patterns at three representative frequencies of 759, 1920, and 2500 MHz for the fabricated antenna. In the azimuthal plane (x - y plane), near-omnidirectional radiation at 759 MHz is seen. While at higher frequencies (1920 and 2500 MHz), the radiation is seen to be stronger in the $+y$ direction than in the $-y$ direction. This is owing to the antenna mounted near the left-hand-side corner of the top edge of the device ground plane in the experiment, which makes the excited surface currents asymmetric on the device ground plane, especially along the top edge of the device ground plane, hence causing asymmetric radiation in the direction along the y direction. It is also observed that both the E_θ and E_ϕ radiation are comparable in the x - y plane, which is advantageous for practical applications where the propagation environment therein is usually complex. In general, the radiation characteristics obtained for the proposed antenna are acceptable for mobile communication applications.

4. CONCLUSION

A new structure of the coupled-fed inverted-F antenna with an inverted-F coupling feed for achieving the dual-wideband operation with a small size has been proposed for the tablet computer applications. With a planar, small-size configuration disposed on one surface of a 0.4-mm FR4 substrate of size $10 \times 40 \text{ mm}^2$, the proposed antenna can provide two wide operations to cover the LTE/WWAN operation in the 704 ~ 960 and 1710 ~ 2690 MHz bands. The obtained dual-wideband operation has been shown to be mainly owing to the shorting strip and the chip capacitor embedded in the feeding strip of the inverted-F coupling feed. Detailed operating principle of the antenna has been discussed. Acceptable radiation characteristics for frequencies in the two wide operating bands for the mobile communication applications have also been obtained. The proposed antenna is especially suitable for slim tablet computer applications.

REFERENCES

1. K.L. Wong, *Planar antennas for wireless communications*, Wiley, New York, 2003.
2. D.L. Huang, H.L. Kuo, C.F. Yang, C.L. Liao, and S.T. Lin, Compact multibranch inverted-F antenna to be embedded in a laptop computer for LTE/WWAN/IMT-E Applications, *IEEE Antennas Wireless Propag Lett* 9 (2010), 838–841.
3. K.L. Wong and W.Y. Chen, Small-size printed loop-type antenna integrated with two stacked coupled-fed shorted strip monopoles for eight-band LTE/GSM/UMTS operation in the mobile phone, *Microwave Opt Technol Lett* 52 (2010), 1471–1476.
4. K.L. Wong, H.J. Jiang, and T.W. Weng, Small-size planar LTE/WWAN antenna and antenna array formed by the same for tablet computer application, *Microwave Opt Technol Lett* 55 (2013), 1928–1934.
5. J.H. Lu and Y.S. Wang, Internal uniplanar antenna for LTE/GSM/UMTS operation in a tablet computer, *IEEE Trans Antennas Propag* 61 (2013), 2841–2846.
6. ANSYS HFSS, Ansoft Corp., Pittsburgh, PA, Available at: <http://www.ansys.com/products/>.
7. C.H. Chang and K.L. Wong, Small-size printed monopole with a printed distributed inductor for penta-band WWAN mobile phone application, *Microwave Opt Technol Lett* 51 (2009), 2903–2908.
8. F.H. Chu and K.L. Wong, Internal coupled-fed dual-loop antenna integrated with a USB connector for WWAN/LTE mobile handset, *IEEE Trans Antennas Propag* 59 (2011), 4215–4221.
9. C.L. Liu, Y.F. Lin, C.M. Liang, S.C. Pan, and H.M. Chen, Miniature internal penta-band monopole antenna for mobile phones, *IEEE Trans Antennas Propag* 58 (2010), 1008–1011.
10. J.H. Kim, W.W. Cho, and W.S. Park, A small dual-band inverted-F antenna with a twisted line, *IEEE Antennas Wireless Propag Lett* 8 (2009), 307–310.
11. K.L. Wong, Y.W. Chang, and S.C. Chen, Bandwidth enhancement of small-size WWAN tablet computer antenna using a parallel-resonant spiral slit, *IEEE Trans Antennas Propag* 60 (2012), 1705–1711.
12. K.L. Wong, T.J. Wu, and P.W. Lin, Small-size uniplanar WWAN tablet computer antenna using a parallel-resonant strip for bandwidth enhancement, *IEEE Trans Antennas Propag* 61 (2013), 492–496.
13. S.H. Chang and W.J. Liao, A broadband LTE/WWAN antenna design for tablet PC, *IEEE Trans Antennas Propag* 60 (2012), 4354–4359.
14. Y.L. Ban, S.C. Sun, J.L.W. Li, and W. Hu, Compact coupled-fed wideband antenna for internal eight-band LTE/WWAN tablet computer applications, *J Electromagn Waves Appl* 26 (2012), 2222–2233.
15. K.L. Wong and T.J. Wu, Small-size LTE/WWAN coupled-fed loop antenna with band-stop matching circuit for tablet computer, *Microwave Opt Technol Lett* 54 (2012), 1189–1193.
16. K.L. Wong, Y.C. Liu, and L.C. Chou, Bandwidth enhancement of WWAN/LTE tablet computer antenna using embedded parallel resonant circuit, *Microwave Opt Technol Lett* 54 (2012), 305–309.
17. T.W. Kang and K.L. Wong, Simple two-strip monopole with a parasitic shorted strip for internal eight-band LTE/WWAN laptop computer antenna, *Microwave Opt Technol Lett* 53 (2011), 706–712.
18. T.W. Kang, K.L. Wong, L.C. Chou, and M.R. Hsu, Coupled-fed shorted monopole with a radiating feed structure for eight-band LTE/WWAN operation in the laptop computer, *IEEE Trans Antennas Propag* 59 (2011), 674–679.
19. T.W. Kang and K.L. Wong, Internal printed loop/monopole combo antenna for LTE/GSM/UMTS operation in the laptop computer, *Microwave Opt Technol Lett* 52 (2010), 1673–1678.
20. K.L. Wong and W.J. Lin, WWAN/LTE printed slot antenna for tablet computer application, *Microwave Opt Technol Lett* 54 (2012), 44–49.
21. K.L. Wong, W.J. Wei, and L.C. Chou, WWAN/LTE printed loop antenna for tablet computer and its body SAR analysis, *Microwave Opt Technol Lett* 53 (2011), 2912–2919.